Sensors & Transducers, Vol. 248, Issue 1, January 2021, pp. 1-9

www.sensorsportal.com

Sensors & Transducers

Published by IFSA Publishing, S. L., 2021
http://www.sensorsportal.com

Thermal and Moisture Dependent Material Characterization and Modeling of Glass Fiber Reinforced Epoxy Laminates

[1, *] Mahesh Yalagach, [1] Peter Filipp Fuchs, [2] Thomas Antretter, [3] Michael Feuchter, [4] Tao Qi and [5] Markus Weber

[1] Polymer Competence Center Leoben GmbH (PCCL), Leoben, Austria
[2] Montanuniversität Leoben, Institute of Mechanics, Leoben, Austria
[3] Montanuniversität Leoben, Institute of Material Science and Testing of Polymers, Leoben, Austria
[4] Austria Technologie & Systemtechnik Aktiengesellschaft, Leoben, Austria
[5] ams AG, Premstätten, Austria
[1] Tel.: + 43 3842 42962 716
E-mail: mahesh.yalagach@pccl.at

Received: 30 November 2020 /Accepted: 31 December 2020 /Published: 29 January 2021

Abstract: The Micro-Electro-Mechanical Semiconductor (MEMS) sensor packages are an advanced multi-material composite system. These packages comprise polymeric materials like prepregs, solder-mask, insulation, and conductive adhesives. Prepregs are glass fiber reinforced epoxy laminates. Only a low material sensitivity to environmental influences will ensure the sensors' reliable performance during their application lifetime. To this end, the potentially applied materials undergo defined thermal and moisture-dependent material characterization. In this contribution, the influence of moisture and temperature has been studied for five different prepreg materials, which are commonly applied as a substrate material in a MEM'S sensor. The measured thermal and moisture dependent material properties are the basis for a numerical diffusion analysis and a virtual hygro-thermo-mechanical reliability assessment.

Keywords: Thermo-mechanical characterization, Hygroscopic swelling, Thermal and moisture expansion, Tensile tests.

1. Introduction

The use of MEMS sensor packages has revolutionized the automotive, home, and building applications (HABA) and Internet of Things (IoT) industries [1, 13]. However, increasing demands on their functionality and reliability necessitates improved packaging materials concerning thermal and moisture changes. The temperature and moisture are the essential parameters associated with the electronic packages' reliability and performance [2]. The materials involved in MEMS sensor packages show significant effects like thermal expansion and hygroscopic swelling when exposed to harsh environmental loads. Due to these effects, during the application of the packages, stresses are introduced.

The induced stresses cause deformation, potentially delamination, and cracks in the materials [4, 11]. In this contribution, the dependence of thermal distribution and moisture absorption in five different prepregs, commonly used in MEMS sensors, is analyzed. The prepreg materials serve as a substrate material for a MEMS sensor build-up. The moisture absorption and thermal mismatch due to the difference in the coefficient of thermal expansion (CTE) of the individual materials significantly impact the MEMS

sensor package reliability [7]. Therefore, the characterization of thermal effects, moisture absorption, and diffusion in these packages need to be accounted for modeling the sensor package's reliability behavior. In doing so, the prepreg materials have been extensively studied using different temperature and moisture dependent material characterization techniques. The obtained moisture and temperature-dependent material properties are prepared to be used in hygro-thermo-mechanical simulations [4, 5] to assess the deformation and stress conditions changes. This information serves as vital information for material and design optimization to eliminate moisture-related failures.

2. Experimental

An extensive thermo-mechanical and hygroscopic material characterization was performed to understand the materials' behavior under different temperature and moisture loads. These characterization techniques involve understanding the thermal distribution, moisture absorption, and its impact on the physical, chemical, and mechanical properties of the prepreg materials. Different thermal and moisture dependent characterization techniques like dynamic mechanical analysis (DMA), thermo-mechanical analysis (TMA), gravimetric humidity conditioning, Coefficient of Moisture Expansion (CME), and humidity dependent Young's modulus were performed. Five different prepregs, CCL-1037, CCL-1078, PP1-1037, PP2-7628 and PP3-1037, were considered for the characterization. They vary in their matrix material, fabric reinforcement type and thickness. The thickness of the prepregs varied from 60 µm to 1.5 mm [13]. The following sections explain briefly the different measurement techniques used:

2.1. Temperature-Dependent Young's Modulus

The temperature-dependent Young's Modulus (E) for the prepreg materials was measured using tensile tests and DMA. The temperature-dependent tensile tests were performed for the defined temperatures 23 °C, 100 °C, 180 °C and 250 °C using Zwick Z010 (Zwick Roell AS, Ulm, Germany) universal test system. The acquisition of strains was performed using the digital image correlation (DIC) method. The measured Young's modulus E was compared with results from Dynamic Mechanical Analysis (DMA) performed using Mettler Toledo DMA (Mettler-Toledo, Columbus, Ohio, USA) in a tensile mode under controlled displacement load. The materials were tested at a frequency of 1 Hz and over a temperature range of -100 °C to 300 °C with a 2 K/min heating rate.

2.2. Thermo-Mechanical Analysis (TMA)

The in-plane CTE was measured using Q400 TCT (Dantec Dynamics, A/S, Skovlunde, Denmark), which utilizes the DIC measurement technique to acquire a change in strain with an increase in temperature. Furthermore, the thermal conductivity $\lambda(T)$ measurements were performed using Light Flash Analysis (LFA). LFA utilizes a non-destructive and contact-free approach to measure the thermal diffusivity $a(T)$. The measurement was performed using – Netzsch LFA 467 HyperFlash® (Netzsch GmbH, Selb, Germany). Based on this approach, the thermal conductivity can be computed using (1):

$$\lambda(T) = a(T)\, c_p\,(T)\, \rho(T), \tag{1}$$

where density $\rho(T)$ and heat capacity $c_p(T)$ were measured using high-resolution balance and differential scanning calorimetry (DSC), respectively. The dimensions of the material samples and test parameters for in-plane CTE and thermal conductivity measurements were considered according to [4, 12].

2.3. Gravimetric Humidity Conditioning

The moisture dependent properties like moisture diffusion coefficient D and saturated mass M_{sat} for the prepregs were measured using the gravimetric humidity conditioning method [5]. Apart from conditioning the prepregs in a distilled water bath [3], a climate chamber was used to measure the moisture uptake at 85 °C and 85 % RH (Relative Humidity) [13]. Before starting the humidity conditioning, the prepregs were conditioned in a temperature oven at 125 °C until they were completely dried (constant weight). To monitor the weight change during the conditioning, the prepregs were repeatedly removed at predefined points in time from the plastic container or the climate chamber. The prepregs' surface was cleaned using paper tissue, and they were weighed using a high precision balance. The prepregs tend to follow single Fickian diffusion law above their glass transition temperature T_g. But, at a temperature below T_g, these materials follow a non-Fickian or dual Fickian diffusion model [7]. In this contribution, the experimental conditioning curves were analytically approximated using single and dual Fickian diffusion models.

2.4. Coefficient of Moisture Expansion (CME)

The hygroscopic swelling strains ε^{β} developed during the gravimetric humidity conditioning are supposed to have a linear relationship with the change in moisture concentration ΔC [5, 13] according to (2):

$$\varepsilon^{\beta} = \beta \Delta C, \tag{2}$$

where β is the CME. The effect of hygroscopic swelling strains ε^{β} in the prepregs is measured using a Digital Image Correlation (DIC) approach. In this process, the hygroscopic strains are monitored during drying at defined temperature levels [4]. The moisture changes or changes in concentration are measured using a high-resolution balance. The CME measurements are carried out on the prepregs, which have reached their maximum mass saturation during the humidity conditioning process. The desorption of the saturated material samples was carried out at 70 °C, 90 °C, 120 °C, 140 °C and 160 °C for six hours. The CME (β) is computed from a linear curve fit between the hygroscopic swelling strains ε^{β} and the change in concentration ΔC.

2.5. Humidity Dependent Young's Modulus

To assess the humidity effects on Young's modulus, humidity-controlled tensile tests were performed on the prepregs [13]. Before the humidity dependent testing, the prepregs were dried in a temperature chamber at 125 °C for 24 hours in the first step and conditioned using a climate chamber in the second step. The defined temperature and humidity levels were 23 °C (50 % and 85 % RH), 60 °C (50 % and 85 % RH) and 85 °C (50 % and 85 % RH). The tests were performed using a Weiss Technik climate chamber and an Instron 4505 universal testing system. For the strain data acquisition, a Mercury 3D DIC system was used.

The dimensions of the tensile specimens were prepared according to ISO 527 – 1BA [14]. Fig. 1 shows the test setup used for the measurement of humidity dependent tensile tests for the prepregs. The Change in Young's modulus (E) due to absorption of moisture was also measured by performing DMA.

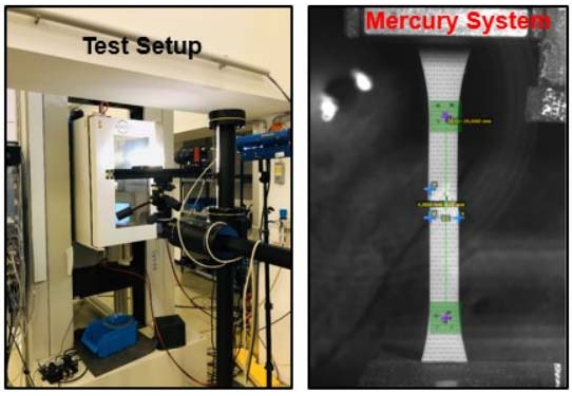

Fig. 1. Experimental setup for the humidity-controlled tensile test with climate chamber and a Mercury 3D DIC system [13].

The prepregs materials pre-conditioned by immersing in distilled water were considered. The saturated materials were subjected to testing in DMA. The testing parameters for DMA measurement remained the same as considered in thermo-mechanical characterization. These DMA measurements were performed for CCL-1078 prepreg materials due to the difficult measurement technique, and the moisture from the conditioned materials are lost during the clamping and stabilization of the measurement system.

3. Verification Simulation

To determine the moisture absorption in prepregs numerically, a verification simulation model was set up in Abaqus (Abaqus 2017, Dassault Systemes Simulia Corp., Providence, USA) using a mass diffusion analysis at test specimen level. As Abaqus uses Fick's law to model the mass diffusion analysis [8, 9], this analysis was numerically solved using a dual Fickian diffusion model approach [3]. The block diagram in Fig. 2 depicts the modeling approach for the verification simulation.

The simulation model is initially started with the heat transfer simulation. The resulting nodal temperature is used in a mass diffusion simulation to access the conditioning's temperature effects as a predefined boundary condition. The mass diffusion model was solved using two parallel single Fickian mass diffusion analyses using the analytically fitted parameters moisture diffusion coefficient D and saturated mass M_{sat} as boundary conditions. The resulting single Fickian moisture concentrations were saved as field variables and were summed up using the USDFLD subroutine. The resulting temperature distribution and moisture concentration were used in a subroutine UEXPAN to compute the total volumetric strains due to moisture uptake and thermal effects.

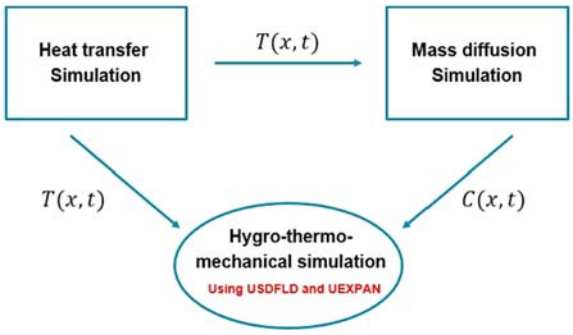

Fig. 2. Verification simulation modeling approach [4].

4. Results and Discussion

The results obtained from thermo-mechanical and hygroscopic material characterization are discussed in this section. Initially, the results obtained for in-plane CTE $\alpha(T)$ and thermal conductivity $\lambda(T)$ are discussed, followed by hygroscopic material characterization results [13].

Fig. 3 shows the in-plane CTE $\alpha(T)$ results obtained for the prepreg materials. The CCL-1037 and CCL-1078 show a similar CTE trend for the overall temperature range of -50 °C to 250 °C. The CCL-1037 has a higher resin content of 27 % than CCL – 1078 (23%). Therefore, CCL-1078 has a lower CTE in the initial temperature range (-50 °C – 150 °C). Also, a lower CTE value was measured for PP1-1037 compared with other materials. The PP2-7628 and PP3-1037 showed a higher CTE value in the initial temperature ramp. On close observation, the CTE values decrease due to T_g for both materials. The CTE values for PP3-1037 is higher than other prepreg materials. Therefore, PP3-1037 is a poor material choice as a substrate in microelectronic packages. The maximum difference of 20 % in all the materials emphasize the importance of the material choice.

Fig. 4 illustrates a wide range of thermal conductivity $\lambda(T)$ values for the considered prepreg materials. The $\lambda(T)$ values measure the ability of the material to conduct heat. The CCL-1037 and CCL-1078 show a similar trend for the measured temperature range.

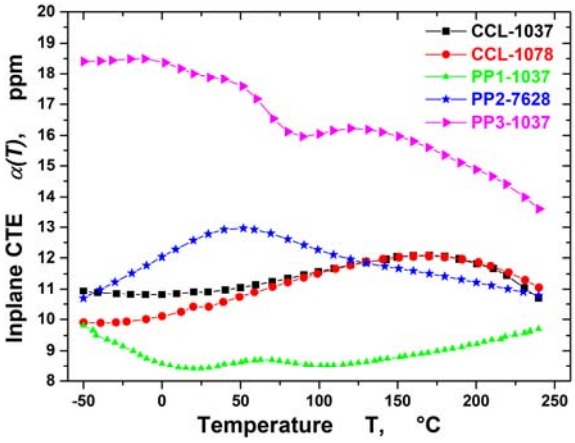

Fig. 3. The in-plane CTE $\alpha(T)$ measured for different prepregs as a function of temperature.

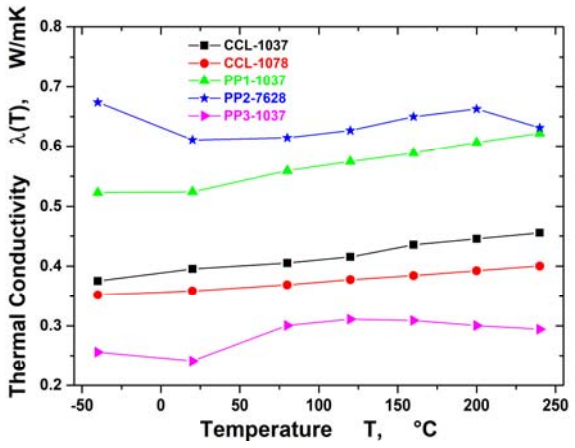

Fig. 4. The thermal conductivity $\lambda(T)$ measured for different prepregs as a function of temperature.

Furthermore, both PP1-1037 and PP2-7628 depict a higher $\lambda(T)$. Heat transfer through these prepreg materials occurs at a higher rate compared with other prepregs. Additionally, PP3-1037 shows relatively lower $\lambda(T)$; this is mainly attributed to this prepregs' substandard matrix material.

The gravimetric humidity conditioning results for prepregs show a temperature and humidity dependent moisture uptake trend for the considered prepregs. Fig. 5 represents the typical moisture uptake curve for the prepregs conditioned at 85 °C and 85 % RH. A maximum moisture uptake of nearly 0.8 % was observed in PP3-1037 material, and a minimum of 0.5 % was found in CCL-1078.

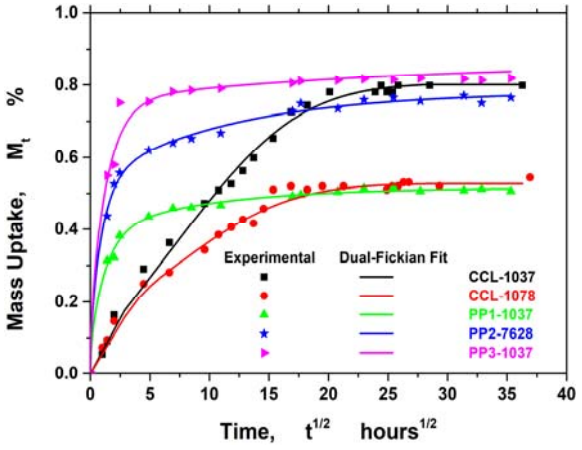

Fig. 5. Typical moisture gain trend and curve fit using an analytical solution (dual Fickian diffusion model) for prepregs at 85 °C and 85 % RH [13].

Figs. 6, 7 and 8 depict the typical moisture gain trend obtained by immersing the prepregs in a distilled water bath and conditioning them at 90 °C, 60 °C and 23°C. The PP3-1037 material absorbed the maximum moisture (1.3 %) compared with other prepreg materials at all conditioning temperatures. This prepreg is made up of substandard matrix material, which tends to absorb more moisture during the humidity conditioning.

Alternatively, a minimum of 0.6 % of moisture absorption was noticed in CCL-1078 material. The prepregs CCL-1037 and CCL-1078 have similar matrix material but differ in their resin content, fabric reinforcement type, and thickness. The absorption of moisture in CCL-1037 is higher than in CCL-1078. The increase in absorption in CCL-1037 is due to the presence of higher resin content than CCL-1078.

The materials PP1-1037 and PP2-7628 have a similar moisture gain trend but differ in maximum moisture absorbed. From Fig. 6 and Fig. 7, a maximum of 0.7 % and nearly 1 % was observed for PP1-1037 and PP2-7628 prepregs, respectively. Consequently, Fig. 5 - Fig. 8 depict that the dual Fickian diffusion model fits the experimental data's overall behavior.

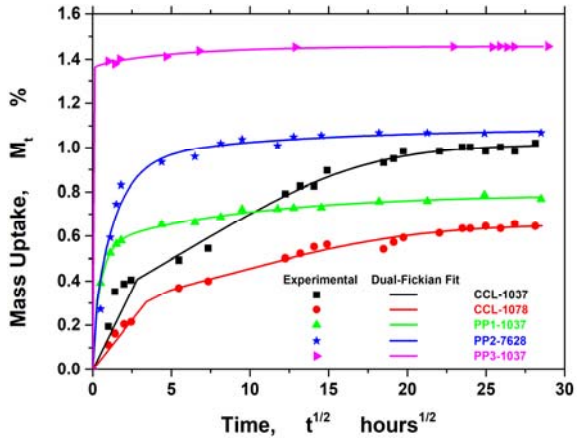

Fig. 6. Typical moisture gain trend and curve fit using an analytical solution (dual Fickian diffusion model) for prepregs at 90 °C immersion [13].

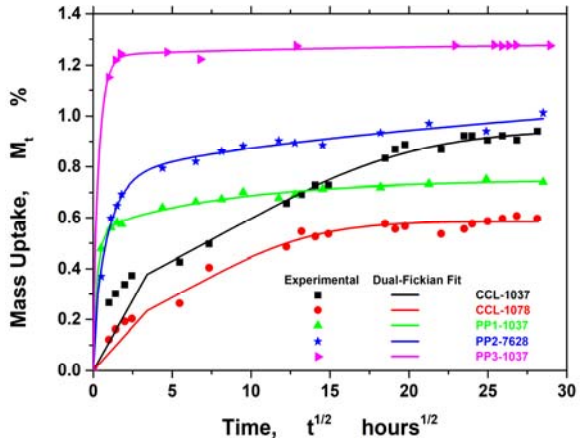

Fig. 7. Typical moisture gain trend and curve fit using an analytical solution (dual Fickian diffusion model) for prepregs at 60 °C immersion [13].

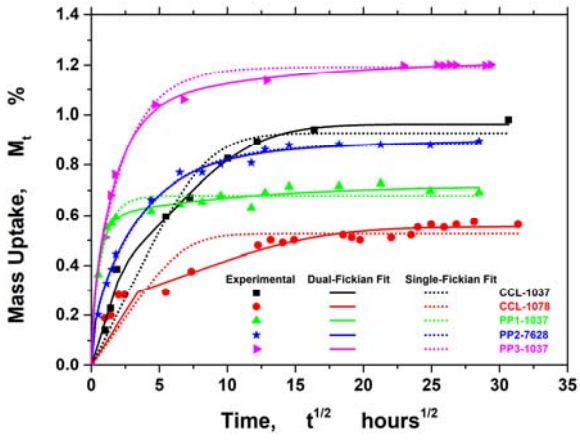

Fig. 8. Typical moisture gain trend and curve fit using an analytical solution (single and dual Fickian diffusion model) for prepregs at 23 °C immersion [13].

Furthermore, in Fig. 8, the dotted lines represent the single Fickian diffusion model's nonlinear fit. The fit from the single Fickian model cannot follow the experimental data trend in the initial region. The obtained saturated mass M_{sat} and the diffusion coefficient D obtained from dual Fickian fit were further used in "Hygro-thermo-mechanical simulations" [4, 5] and in the verification simulation model to compute the total concentration change numerically. To summarize, from the typical moisture gain trend, both the diffusion coefficient and saturated mass increase with an increase in temperature and humidity.

For the Coefficient of Moisture Expansion (CME), the change in concentration ΔC measured using desorption or drying process is depicted in Fig. 9. It can be observed that the prepreg PP3-1037 and PP2-7628 show the highest concentration change of nearly 1.2 % compared with PP1-1037 (0.8 %), CCL-1078 (0.6 %) and CCL-1037 (1 %).

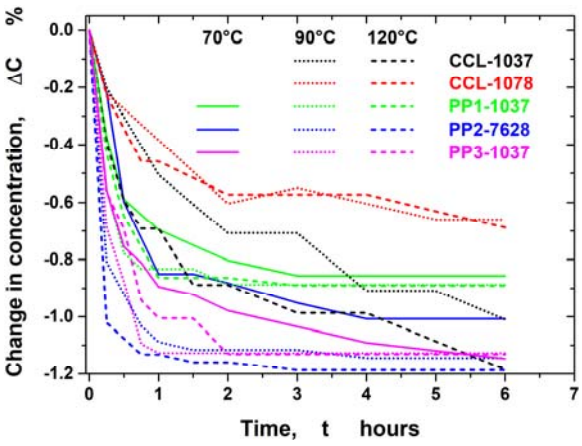

Fig. 9. Change in moisture concentration ΔC for prepregs from the desorption process at 70 °C, 90 °C and 120 °C for six hours [13].

The moisture desorption concentration trend is in good agreement with the moisture absorption trend (Fig. 5 - Fig. 8) during the gravimetric humidity conditioning.

The desorption measurements were also carried out at 140 °C and 160 °C for six hours.

The measured hygroscopic swelling strains ε^{β} for the prepregs are depicted in Fig. 10. The swelling strains are very low for all the prepregs considered. However, significant shrinkage of 0.12 % was observed for prepreg PP2-7628 at 70 °C. Moreover, the CCL-1037 and CCL-1078 did not show any hygroscopic swelling strains at all conditioning temperatures. Henceforth, the desorption and hygroscopic swelling measurements were not performed at 70 °C. The prepreg PP2-7628 and PP3-1037 follow a similar temperature trend, i.e., the swelling strains decrease with an increase in temperature. Conversely, PP1-1037 shows the opposite trend. This effect is mainly caused by the different glass transition temperature (T_g) regions for the prepregs. The prepregs PP1-1037, PP2-7628 and PP3-1037 have a T_g of 270 °C, 170 °C and 150 °C, respectively.

While the considered conditioning temperatures to measure CME is below the T_g level for PP1-1037, they are within the onset of the transition region for PP2-7628 and PP3-1037. Therefore, a different temperature dependence trend can be observed for these materials [8].

The computed CME (β) at different temperatures for the prepregs is depicted in Fig. 11. As the prepregs CCL-1037 and CCL-1078 did not show any swelling strains, no CME is presented for these materials in the figure. The figure also depicts the decrease in CME's value with an increase in temperature for PP2-7628 and PP3-1037. The decrease is mainly in the glass transition region for both the prepregs.

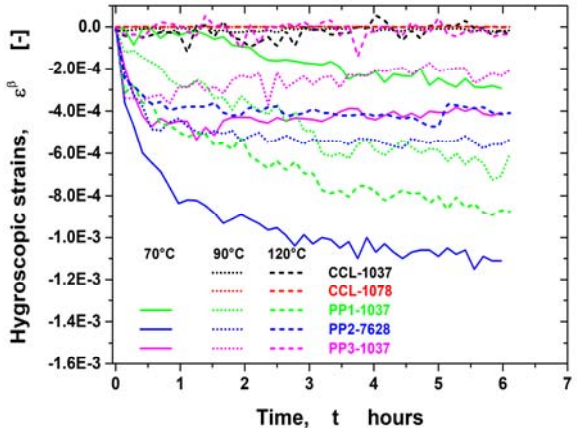

Fig. 10. The measured CME at different temperatures for the prepregs [13].

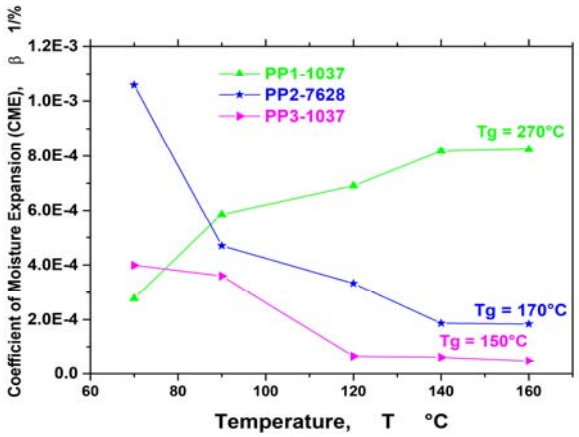

Fig. 11. The measured CME at different temperatures for the prepregs [13].

The results obtained from humidity-controlled tensile tests for the considered prepregs are presented exemplarily. They are compared against the results from thermo-mechanical DMA, the temperature-controlled tensile test results. (See Figs. 12-16). The solid lines in Fig. 12 - Fig. 16 represent the DMA curve measured at 1 Hz, the square symbols represent Young's moduli measured using a temperature oven, and the dot symbols and the star symbols represent Young's moduli measured using a climate chamber with a controlled humidity level of 50 % RH and 85 % RH respectively.

Overall, Young's moduli E obtained from temperature-controlled tensile tests are in good agreement with DMA results at increased temperatures for the prepregs considered for both Warp (0°) and 45° test specimens. Discrepancies at room temperature for CCL-1037, CCL-1078, PP2-7628 and PP3-1037 can be attributed to possible unstable humidity conditions when not using the climate chamber.

To quantify relative humidity effects, the prepregs were tested at 50 % RH and 85 % RH conditions at temperature levels of 23 °C, 60 °C and 85 °C. A decrease in Young's moduli E for all the prepregs was observed at 50 % RH and 85 % RH, respectively, at all considered temperature levels.

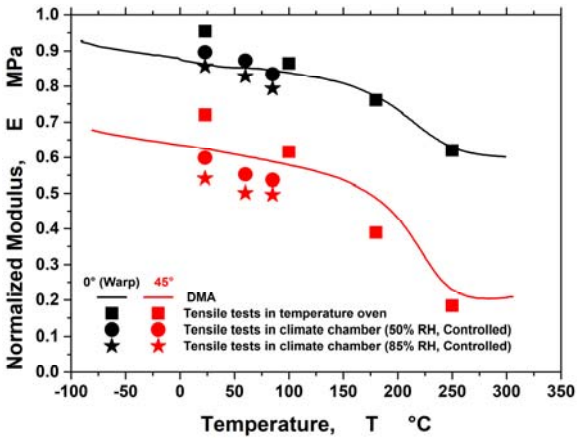

Fig. 12. Comparison of controlled humidity tensile tests with DMA and tensile tests in temperature oven for CCL-1037 prepreg (normalized to maximum modulus) [13].

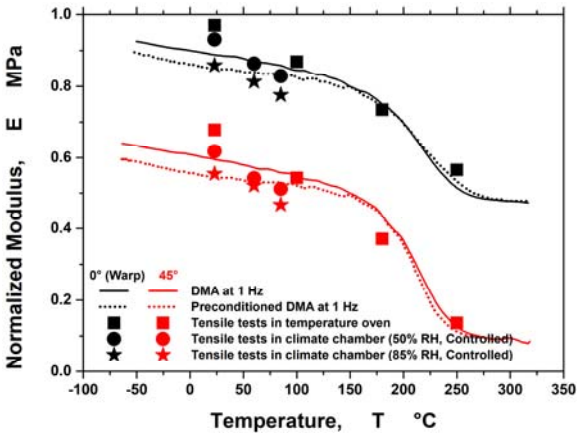

Fig. 13. Comparison of controlled humidity tensile tests with DMA and tensile tests in temperature oven for CCL-1078 prepreg (normalized to maximum modulus) [13].

This decrease is mainly attributed due to the presence of moisture in the prepregs during the humidity conditioning. The Young's modulus E value

for 85 % RH is relatively smaller than E at 50 % RH. The lower value of *E* is mainly due to the presence of higher moisture content at 85 % RH than at 50 % RH at the same temperature. This hydration difference explains the difference as excess moisture lowers the mechanical strength and stiffness of the prepregs. An increased humidity level leads to a reduced stiffness.

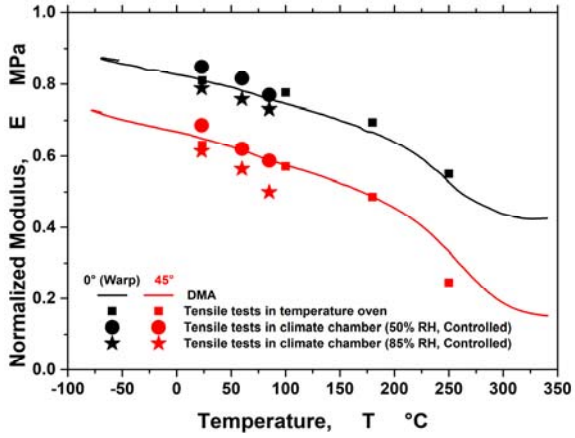

Fig. 14. Comparison of controlled humidity tensile tests with DMA and tensile tests in temperature oven for PP1-1037 prepreg (normalized to maximum modulus) [13].

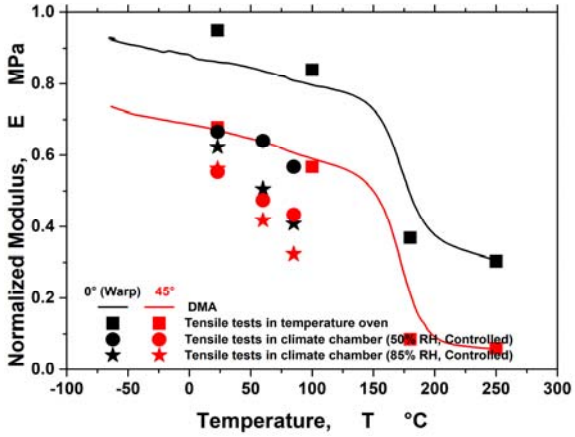

Fig. 15. Comparison of controlled humidity tensile tests with DMA and tensile tests in temperature oven for PP2-7628 prepreg (normalized to maximum modulus) [13].

The Young's Modulus E obtained by performing DMA of the pre-conditioned material (CCL-1078) is shown in Fig. 13 with black (0°) and red (45°) dotted lines. CCL-1078 absorbs nearly 0.6 % of moisture during the pre-conditioning using gravimetric humidity conditioning. A deviation in the Young's moduli values of 1 % in the temperature range of -80 °C – 150 °C was observed for both 0° and 45° directions test specimen. Furthermore, the increase in temperature from 150 °C desorbs moisture in the specimen. Therefore, the modulus *E* above 150 °C follows the DMA trend at 1 Hz without any pre-conditioning. Additionally, Young's moduli measured by DMA are in close agreement with those from humidity-controlled tensile tests.

The prepreg PP2-7628 is most commonly used in MEMS and PCB manufacturing. This prepreg has a higher resin content compared with other prepreg materials. Therefore, this material absorbs more moisture and affects the material's strength by lowering Young's moduli *E* (see Fig. 15 for 0° (Warp)) compared with DMA and temperature-controlled tensile results tests.

Fig. 16 shows the tensile test results obtained for PP3-1037. The temperature-controlled tensile tests were only performed at room temperature of 23 °C. Therefore, the results from humidity dependent tensile tests are compared with *E* values at 23 °C and with DMA along 0° (Warp) and 45° test specimens.

The results from the verification simulation have been depicted in Fig. 17.

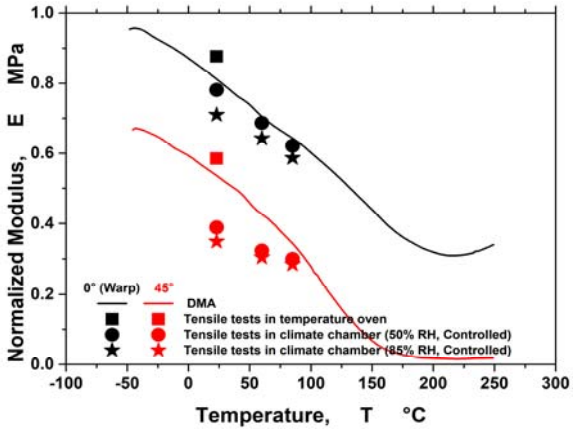

Fig. 16. Comparison of controlled humidity tensile tests with DMA and tensile tests in temperature oven for PP3-1037 prepreg (normalized to maximum modulus) [13].

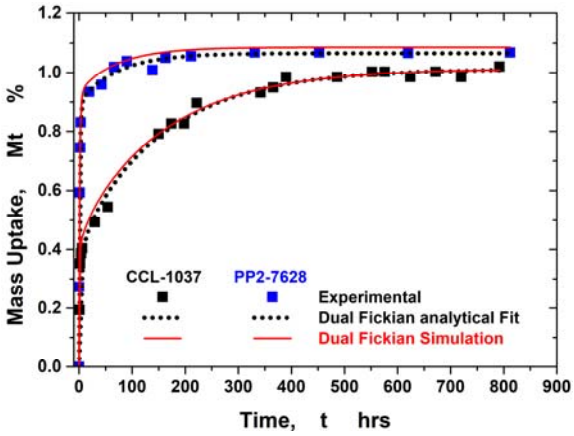

Fig. 17. Comparison of moisture absorption curve between experimental, analytical, and numerical simulation using humidity conditioning simulation for CCL-1037 and PP2-7628 [13].

The verification simulation was performed at the specimen level for the prepregs immersed in a distilled water bath and conditioned at 90 °C. The solid red

lines represent the result obtained from a verification simulation; the black dotted lines represent the curve from the analytical fit, and the black and blue squared symbols represent the experimental humidity conditioning curves for CCL-1037 and PP2-7628, respectively. The verification simulation using the dual Fickian diffusion model agrees with both experimental and analytical fit curves' overall behavior. Therefore, this verification simulation model serves as a basis to the hygro-thermo-mechanical modeling [4, 5] approach. The verification simulation was also performed for all the five prepregs considered in this contribution. Overall, the simulation results agree with the experimental data and the analytically fit parameters for all the prepregs.

5. Conclusions

In this research work, the results from thermo-mechanical and hygroscopic material characterization for five different prepreg materials are presented. The thermal material properties like in-plane CTE $\alpha(T)$ and thermal conductivity $\lambda(T)$ help predict the right material choice for the substrate in microelectronic packages. Based on the experimental gravimetric conditioning for all the prepregs, a dual Fickian moisture diffusion model was defined. The measured moisture diffusion coefficient D and saturated mass M_{sat} are in good agreement with the analytical fit and verification simulation.

Furthermore, the measured in-plane CTE $\alpha(T)$ and calculated CME values β serve as a material property to analyze the thermal and moisture mismatch in the MEMS sensor package in further reliability studies. The measured humidity and temperature-dependent Young's moduli provide critical information on shifts in the prepregs' mechanical properties due to moisture absorption and thermal distribution, respectively. The measured experimental data will be used in a numerical simulation to determine the moisture and temperature-induced deformation and stresses in a MEMS sensor package. Thereby the measured material behavior is the crucial basis for a reliable sensor system design.

Acknowledgments

The research work was performed within the K-Project "PolyTherm" at the Polymer Competence Center Leoben GmbH (PCCL, Austria) within the framework of the COMET-program of the Federal Ministry for Transport, Innovation, and Technology, and the Federal Ministry for Digital and Economic Affairs with contributions by the University of Leoben, ams AG and by AT&S Austria Technology & Systemtechnik Aktiengesellschaft. Funding is provided by the Austrian Government and the State Government of Styria.

References

[1]. Stellrecht E., Han B., Pecht M. G., Characterization of the hygroscopic swelling behavior of mold compounds and plastic packages, *IEEE Transactions on Components and Packaging Technologies*, Vol. 27, Issue 3, 2004, pp. 499-506,

[2]. Kim H., *et al*., Investigation of moisture-induced delamination failure in a semiconductor package via multi-scale mechanics, *Journal of Physics D: Applied Physics*, Vol. 44, 2011, 034007.

[3]. Y. He, *et al*., In-situ Characterization of Moisture Absorption and Desorption in a Thin BT Core Substrate, in *Proceedings of the 57th Electronic Components and Technology Conference (ECTC'07)*, Reno, NV, 2007, pp. 1375-1383.

[4]. M. Yalagach, *et al*., Influence of environmental factors like temperature and humidity on MEMS packaging materials, in *Proceedings of the 7th Electronic System-Integration Technology Conference (ESTC)*, Dresden, 2018, pp. 1-6.

[5]. M. Yalagach, *et al*., Numerical Analysis of the Influence of Polymeric Materials on a MEMS Package Performance Under Humidity and Temperature Loads, in *Proceedings of the IEEE 69th Electronic Components and Technology Conference (ECTC)*, Las Vegas, NV, USA, 2019, pp. 2029-2035.

[6]. JESD22-A120A, Test method for the measurement of moisture diffusivity and water solubility in organic materials used in electronic devices, JEDEC Standards, 2001.

[7]. L. Masaro, X. X Zhu, Physical models of diffusion for polymer solutions, gels and solids, *Progress in Polymer Science*, Vol. 24, Issue 5, 1999, pp. 731-775.

[8]. E. H. Wong, Y. C. Teo, T. B. Lim, Moisture diffusion, and vapor pressure modeling of IC packaging, in *Proceedings of the Electronic Components and Technology Conference*, 1998, pp. 1372-1378.

[9]. Macdonald D. D., 1977, The Mathematics of Diffusion, in: Transient Techniques in Electrochemistry, *Springer*, Boston, MA. https://doi.org/10.1007/978-1-4613-4145-1_3.

[10]. Brewis D. M., Comyn J., Tredwell S. T., Diffusion of water in some modified phenolic adhesives, *Int. J. Adhesion and Adhesives*, Vol. 7, Issue 1, 1987, pp. 30-32.

[11]. Fuchs P. F., Pinter G., Fellner K., Local damage simulations of printed circuit boards based on in-plane cohesive zone parameters, *Circuit World*, Vol. 39, Issue 2, 2013, pp. 60–66.

[12]. Morak M., Marx P., Gschwandl M., Fuchs P. F., Pfost M., Wiesbrock F., Heat Dissipation in Epoxy/Amine-Based Gradient Composites with Alumina Particles: A Critical Evaluation of Thermal Conductivity Measurements, *Polymers*, Vol. 10, Issue 10, 2018, 1131.

[13]. M. Yalagach, *et al*., Characterization and Modeling of Prepregs Applied in MEMS Sensor Packages with a Focus on Moisture Dependence, in *Proceedings of the 3rd International Conference on Microelectronic Devices and Technologies (MicDAT' 2020)*, 22-33 October 2020, pp. 5-10.

[14]. ISO 527-1:2019, Plastics – Determination of tensile properties – Part 1: General principles.